https://doi.org/10.5194/tc-2021-337
Preprint. Discussion started: 20 December 2021

The Cryosphere Discussions
Open Access
EGU

Geophysical measurements of perennial snow patches in Pirin Mountain, Bulgaria

Atanas Kisyov[1], Christian Tzankov[1], and Gergana Georgieva[2]

[1]University of Mining and Geology "Sv. Ivan Rilski", Sofia, Bulgaria
[2]Sofia University "Sv. Kliment Ohridski", Sofia, Bulgaria

Correspondence: Gergana Georgieva (ggeorgieva@phys.uni-sofia.bg)

Abstract. Perennial snow patches are considered as indicators of permafrost occurence. There are no large glaciers on the territory of Bulgaria but small patches of snow and firn have been observed in the high mountains at the end of the summer. In this paper we present results from the first detailed geophysical investigations of Snezhnika microglacier, considered as the southernmost microglacier in Europe. It is situated in the Golyam Kazan cirque, Pirin Mountain, Bulgaria. Ground penetrating radar (GPR) and 2D Electro Resistivity Tomography (ERT) were used to estimate the thickness of the perennial snow patch as well as its subsurface structure. Measurements started in 2018 and continued over the next three years in order to evaluate changes in the snow patches' size and thickness. The mean thickness of Snezhnika is about $4-6\ m$, reaching up to $8\ m$ in some areas. ERT measurements of the deeper parts of the microglacier beds show high electrical resistivities reaching over $60000\ \Omega m$ at a depth of $4-10\ m$. An anomaly at this depth is likewise distinguishable on the GPR profiles. These anomalies are interpreted as frozen zones and are consistently observed on the ERT and GPR profiles in the next two years of the study. These results imply for the first time the existence of permafrost in Pirin mountain and respectively in Bulgaria.

1 Introduction

Perennial snow patches are defined as snow fields existing for at least two consecutive summers (Watanabe, 1988). 82% of the glaciers are smaller than $0.5\ km^2$ and cover 21% of the Earth's total glaciated area (Zemp, 2006). Despite their small size, perennial snow patches and microglaciers are an important object of study for their vital role as water reservoirs for many downstream ecosystems (Milner et al., 2009; Barry et al., 2011). They are sensitive to climate change although they are less influenced by global changes than glaciers. Perennial snow patches survive as a result of avalanching, wind-drift snow and shading (Grunewald et al., 2010). Together with microglaciers they are important also for estimating permafrost areas in high mountains as permafrost is the last stage of the glacial life cycle (Hughes, 2014, 2018).

There are no large glaciers on the territory of Bulgaria since the end of the Little Ice Age, but small patches of snow and firn have been observed in the high parts of the Rila and Pirin Mountains in the end of the summer. Most well studied perennial snow

https://doi.org/10.5194/tc-2021-337
Preprint. Discussion started: 20 December 2021


The Cryosphere Discussions

patch in Bulgaria is Snezhnika (Gruenewald and Scheithauer, 2008; Gachev et al., 2016). It is the modern remains of the Vihren glacier in the Pirin Mountain, varying in size between $0.02\ km^2$ and $0.07\ km^2$ (Gachev, 2017a). The first measurements of its size are made in the 1960's (Popov, 1964); systematic measurements are conducted every year in the end of summer since 1994 (Gruenewald et al., 2008; Gachev, 2016). The size of the microglacier is well monitored but information about its thickness is sparse. In October 1957, Popov (1962) bores into the middle part of Snezhnika and reaches ground at $8\ m$. He also estimates the structure as follows: the upper $80-100\ cm$ represent an icy layer or icy crust which is under direct influence of the surface temperatures. Beneath this layer is firn consisting of grain sizes between 1 and $2\ cm$, increasing with depth. In the end of summer 2006, depth measurements were carried out again and three boreholes were made. The depth in two of them was estimated to be $11\ m$ (Gruenewald et al., 2008). Geophysical measurements were not carried out until 2018 (Georgieva et al., 2019).

Permafrost is a section of the subsurface in which the temperature is continually below $0°$C for at least two years (Harris et al., 1988; Washburn, 1979). The definition is based exclusively on the temperature regime, and thus permafrost can exist in any type of sediment or rock (Ingeman-Nielsen, 2005). Permafrost is also good indicator for climate change (Fort, 2015). The highest amplitude of temperature increase will first be visible in high mountains. Therefore, mountain slopes with permafrost areas are significantly vulnerable to climate change. Thawing of permafrost decreases the stability of slopes and can affect infrastructure in mountain regions. According to Gruber et al. (2009) there are two types of surface phenomena indicating the presence of permafrost in mountains - rock glaciers and other creep phenomena and hanging glaciers and ice faces. Damm et al. (2006) gives geomorphological indicators for mountain permafrost, among which are perennial snow patches. Perennial snow patches contribute to local permafrost occurrence because they work as a shield with relatively high albedo, protecting the frozen underground from heat flux in summer. The existence of many perennial snow patches in an area in the mountains indicates a wider distribution of permafrost, especially in the shade of surrounding peaks (Haeberli, 1975; Rolshoven, 1982). Although there are high mountains reaching almost 3000 m in Bulgaria with suitable conditions for the presence of permafrost (Dobinski, 2005), there is low number of studies on this topic (Onaca et al. (2020)). No publications have been found to investigate the long-term state of the frozen subsurface in high mountains in Bulgaria.

With the development of modern technologies and in particular the equipment used in exploration geophysics, high-quality in-depth information can now be obtained. Geophysical techniques such as electrical resistivity tomography (ERT), and ground-penetrating radar (GPR) are widely used today for a multi-dimensional investigation of subsurface conditions in permafrost environments and corresponding landforms. Until the late 1980's, they were mostly applied in polar regions (see the review by Scott et al. (1990)). The ERT technique is one of the basic methods for permafrost evidence and studies. Geophysical methods are applied also in glacial studies and the GPR technique is most important for the imaging of glacial subsurface conditions (Navarro et al., 2009) and internal glacial structure (Arcone, 1996).

The application of geophysical methods in mountain permafrost regions is related to changes of the physical properties of earth material mainly associated with the freezing of incorporated water. The degree of change in the physical properties depends on water content, pore size, pore water chemistry, ground temperature and pressure on the material (Hoekstra et al.,

https://doi.org/10.5194/tc-2021-337
Preprint. Discussion started: 20 December 2021

1973; King, 1984; King et al., 1988; Hoekstra et al., 1974; Scott et al., 1990). When applied on permafrost, most geophysical methods detect parameters correlated to ice content (Hauck et al., 2001) like high electrical resistivities (ERT).

Using geophysical methods, the structure, depth and extent of frozen areas beneath and near the snow field can be determined relatively quickly and easily, as well as the location of accompanying snow bodies and karst formations (Scott et al., 1990; Dimovski et al., 2015, Georgieva et al., 2019; Kisyov et al., 2018).

Ground-penetrating radar (GPR) is a high-resolution geophysical technique based on the propagation of electromagnetic (EM) waves. Dry snow and ice provide the optimal permittivity conditions of the radar signal from all possible geological environments for georadar pulses with a main frequency above 1 MHz. This is due to the extremely low degree of signal attenuation, which is a result of the low conductivity and the absence of any dielectric or magnetic relaxation processes above this frequency. The successful application of GPR in glaciology is related to the peculiar dielectric properties of frozen materials and to their large contrast with other geological materials (Evans, 1965; Fitzgerald et al., 1975). Employing high-frequency GPR antennas (> 400 MHz) good results can be obtained in delineating the internal structure of perennial snow patches or permafrost zones (Annan et al., 1976; Berthling et al., 2000; Hinkel et al., 2001; Jørgensen et al., 2007; Gadek et al., 2008; Onaca et al., 2015). The advantages of GPR are that data acquisition and processing are relatively fast and the interpretation result can be focused on different depths and scales, with a variety of antenna configurations and frequencies (Pipan et al., 1999; 2000; van der Kruk et al., 2003; Jol, 2009; Zhao et al., 2015; 2016).

On the other hand, snow and ice are an ideal environment for exploration, as stratigraphically they are made up of horizons with good endurance and characteristic shapes. The polar ice sheets may contain layers of basal sea ice several to hundreds of meters thick (Blindow, 1994), while glaciers from temperate continental belts may contain layers rich in dust, sand, or rock debris from a few millimeters to tens of meters (Arcone et al., 1995; Lawson et al., 1998). The perennial snow patches in high mountains are similar to mountain glaciers (as remnants of them) and also contain layers of rock material between thin layers of ice and firn (Kawashima et al., 1993).

Electrical resistivity method (ERT) or 2D Electrotomography is based on the changes in the electrical properties of rocks, both vertically and horizontally using different electrode circuits (Dimovski et al., 2007). Changes in electrical resistivity depend not only on changes in lithology but also in relation to the presence of water in the cracks and pores of the rocks (Dimovski et al., 2015; Hoekstra et al., 1973; Olhoeft, 1978). The decrease in temperature leads to a decrease in electrolytic activity and hence a decrease in conductivity. This effect is significant below the freezing point. This is the reason why the ERT can successfully be applied for studying glacial structures and frozen subsurface areas in mountain regions.

A marked increase in resistivity at the freezing point was shown in several field studies (Supper et al., 2014; Hilbich et al., 2009; Emmert et al., 2017; Hauck, 2013; Kneisel et al., 2007; Kneisel et al., 2008; Mauer et al., 2007; Ikeda, 2006; Hausmann et al., 2012; Onaca et al., 2015). In most permafrost materials, electrolytic conduction takes place, where the current is carried by ions in the pore fluids of the material. In poor conductors with few carriers, such as ice, a slight displacement of electrons with respect to their nuclei produces a dielectric polarization of the material, leading to displacement currents (Telford et al., 1990).

https://doi.org/10.5194/tc-2021-337
Preprint. Discussion started: 20 December 2021

In 2018, 2019 and 2020 geophysical measurements were conducted by the team in two places in Pirin Mountain - Golyam Kazan cirque and Banski Suhodol valley. The aim was to investigate the thickness, internal structure of perennial snow patches and subsurface structure near them. Geophysical measurements in Golyam Kazan cirque were made in three consecutive years and results are presented in this paper.

2 Methods

Geophysical measurements near Snezhnika microglacier include ground penetrating radar (GPR) and 2D Electro Resistivity Tomography (ERT). GPR profiles are crossing the microglacier, while ERT profiles lie between the ice body and the front moraine. Digital elevations model (DEM) with resolution 7.63 cm/pix was also constructed using drone photogrammetry.

2.1 Study site description

Pirin Mountain is a crystalline horst which is part of Rila-Rhodope massif located in southwestern Bulgaria. The studied site is situated in the northern part of the mountain, around the highest peak Vihren (2914 m). The marble that makes up the steep ridges lends the relief its characteristic appearance (Boyadjiev, 1959). Snezhnika microglacier (Gruenewald et al., 2008) is situated in the Golyam Kazan cirque, in Pirin Mountain, noted as the southernmost perennial snow patch in Europe (Grunewald et al., 2010; Gachev 2017a). The location of Snezhnika is determined by the morphological features of the Golyam Kazan cirque, formed between the eastern slope of Vihren Peak (2914 m) and the southern slope of Kutelo Peak (2908 m) (Fig. 1), at around 2400 m asl. It is open to the east, with dimensions of 1200 by 1250 m and an surface of about 1.2 km^2. The western and southern parts of the cirque are outlined by the steeper slope of Vihren Peak and Dzhamdzhiev ridge. The morphology of this slope, and in particular the morphology of the Vihren wall, at the base of which the snow patch is located, favors the accumulation of snow masses through avalanches and shading. The Vihren wall rises west of the snow patch and 420 m above its surface. The wall has mainly eastern exposure and partly northern exposure with slopes from 55 to 65° (almost half of its area). The largest slopes, reaching in places from 85 to 90°, are characteristic of the lower part of the wall. They were formed during the final phase of the last (Wurm) glaciation (Popov, 1962, 1964).

The size of Snezhnika microglacier varies from year to year as it is visible on Fig. 2 but no trend can be determined (Gachev, 2016). Therefore, it cannot be said whether its size decreases or increases starting from the first measurements in 1994 (Gachev, 2016). During the period in which the presented study was conducted (2018-2020) the size of Snezhnika decreased. This made it possible to make ERT profiles on the same place in microglacier's bed where GPR profiles were made in the previous year.

2.2 Ground-penetrating radar

Measurements in Pirin Mountain were carried out using a GPR system, including a SIR-3000 control unit and 270 MHz antenna model 5104A by GSSI, Inc. USA. The settings used are listed in Table 1. By default, all radargrams are processed with the following processing levels:

https://doi.org/10.5194/tc-2021-337
Preprint. Discussion started: 20 December 2021

The Cryosphere Discussions
Open Access
EGU

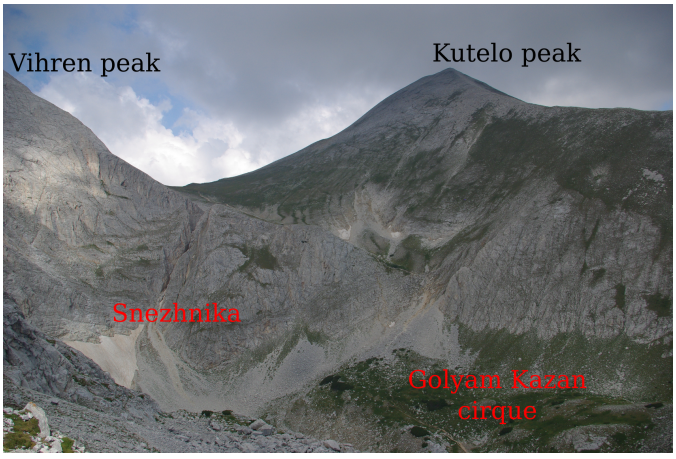

Figure 1. Snezhnika microglacier in Golyam Kazan cirque, surrounded by the highest peaks in Pirin Mountain. Picture is taken from Dzhamdzhiev ridge.

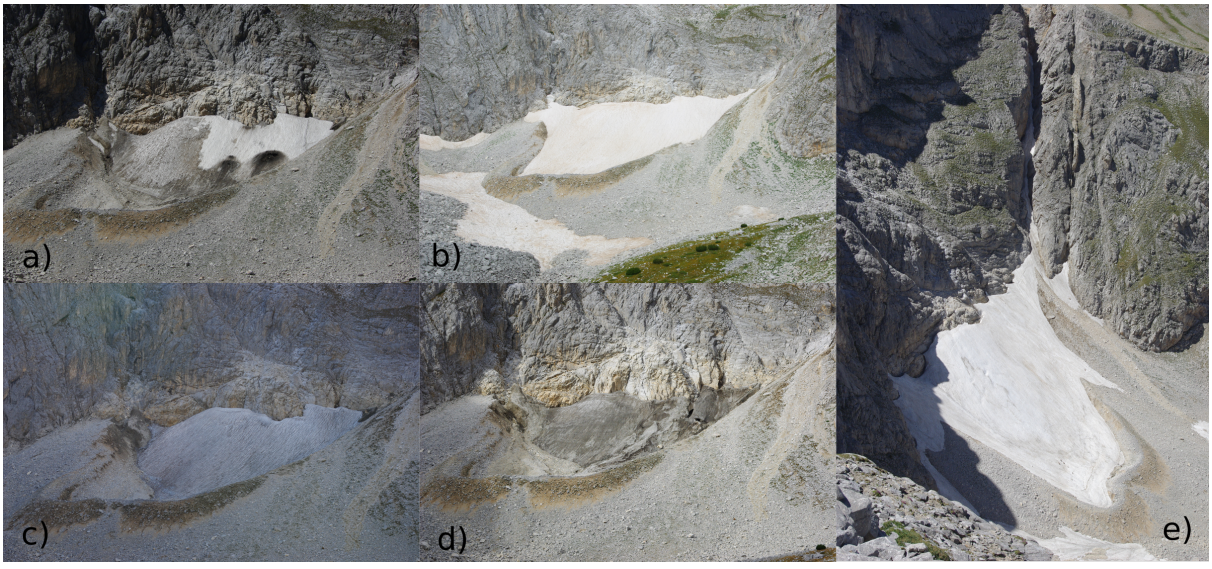

Figure 2. Snezhnika microglacier in Golyam Kazan in years (a) 2017, August 25; (b) 2018, August 25; (c) 2019, October 5 and (d) 2020, October 9. Well visible is decrease of its size between 2018 and 2020 when geophysical measurements were made. Picture e) is taken from the Dzhamdzhiev ridge (near Vihren peak) on 01 July 2017. The shading of the ridge is already visible.

– Pre-processing and geometrization of the radargrams (profiles lengths adjustments; orientation flip; declipping of extreme values and multiplying by scaling factor 1.44; dewow by subtracting mean value at 4 ns time window; resampling the data in x-direction by 2.5 cm trace increment; fixing the zero level by cutting the time section where waves pass through the air before the ground surface)

https://doi.org/10.5194/tc-2021-337
Preprint. Discussion started: 20 December 2021

Table 1. GPR Settings of the measurements.

SURVEYPARAMETERS	2018	2020
Scans per meter	40	20
Samples per scan	1024	512
Time window	210 ns	300 ns
Automatic gain	4 pts	4 pts

IIR Filters Vertical: LP = 700 MHz HP = 75 MHz

- Standard filtration and smoothing (cosine-tapered bandpass filter with low cut frequency 50 MHz, lower plateau 75 MHz, upper plateau 550 Mhz and high cut frequency 750 MHz; 2d median xy-filter on a 5 traces by 5 samples window)
- Signal amplification (profiles normalizing by energy equalization of the parallel profiles; profile trace normalize in order to produce mean amplitude equality distribution for all traces)
- Eliminate horizontal reverberations (applying a background removal filter)

For inverting and interpreting of GPR data the following generalized lithological media with their estimated mean velocities taken from standard properties tables were used in the radargram models: ice 0.15 m/ns, gravel with ice 0.13 m/ns, limestone 0.12 m/ns (Baker et al., 2007).

GPR profiles within this study were made in 2018 and 2020. Locations are presented on Fig. 3. Coordinates of profiles were recorded with Garmin GPSMAP 64st and Garmin GPSMAP 66s with error in horizontal coordinates $1-2$ m. All profiles from 2018 are perpendicular to the slope and follow the relef's horizontals. The first one - GPR(2018)-01, is located in the lowest and comparatively flattened section of the microglacier, and the last, GPR(2018)-05, was in the highest elevation area accessible without additional security. Two profiles from 2020 were situated along the slope and two were in the lower part of the microglacier's bed between head moraine and ice. In 2018 this area was covered by snow (Fig. 2). In order to simplify the processing and the interpretation, all radargrams, except GPR(2020)-3 and GPR(2020)-3, have no topography and are with zero reference level in the elevation axis. The location of the profiles parallel to the slope allowed determining the depth of the ice in the upper parts of the snowfield. Due to the steep slope, laying profiles perpendicular to the slope in this part is extremely difficult.

2.3 Electrical resistivity method

Based on the measurements conducted in different areas of Europe (Supper et al., 2014; Hauck et al., 2001; Mauer et al., 2007; Ingeman-Nielsen, 2005), we determined the most suitable parameters of the measuring scheme for optimal results with permafrost. Measurements in Pirin mountain were carried out using 24 electrodes connected to a resistivity meter (ABEM SAS 1000). The measurements were obtained by combinations of systematic changes in the location of the four active electrodes. The depth of the study depends on the distance between the electrodes and the geometry of the circuit, the gradual increase

https://doi.org/10.5194/tc-2021-337
Preprint. Discussion started: 20 December 2021

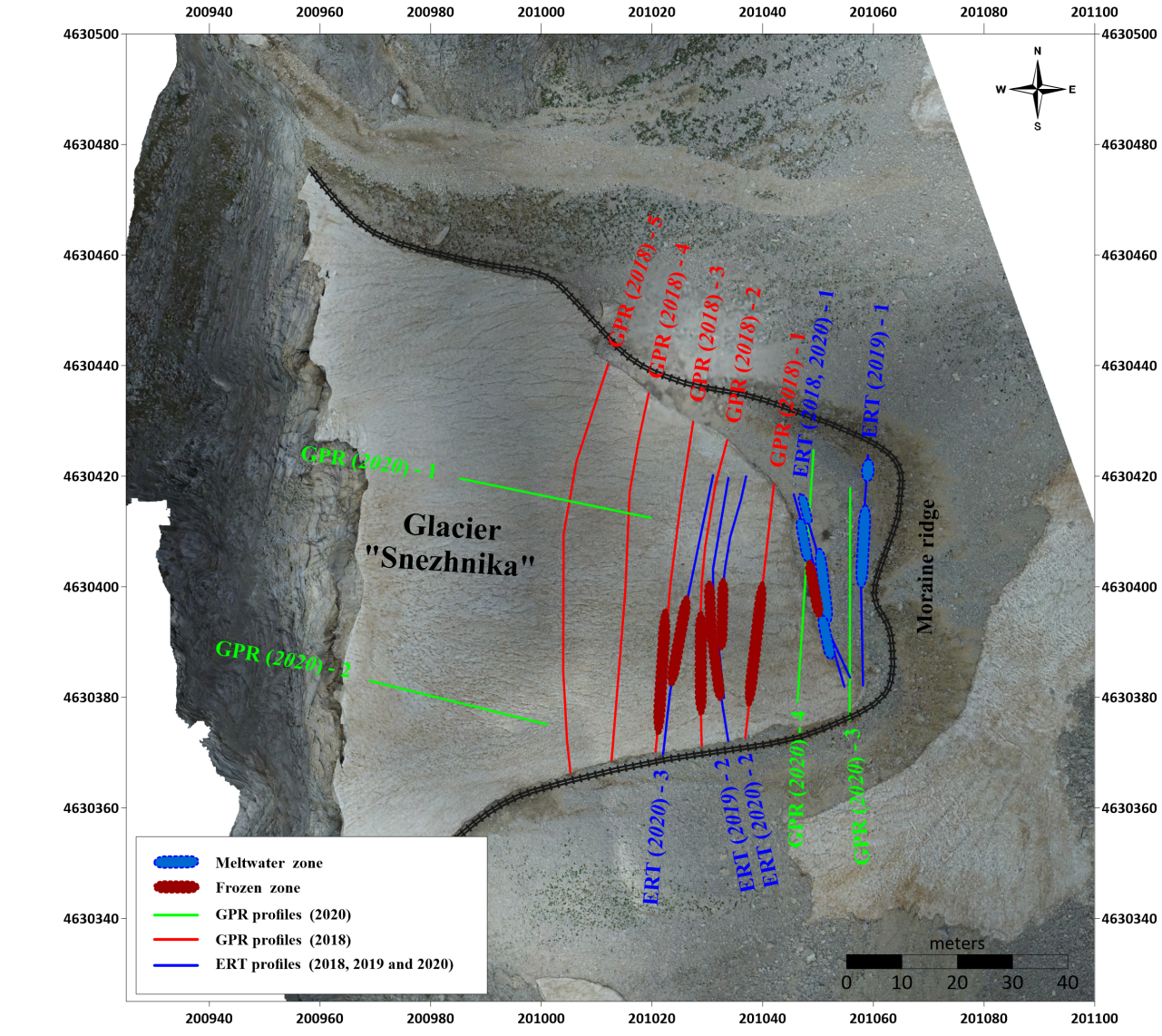

Figure 3. Location and direction (labels are on the starting point) of the all GPR (red for 2018 and green for 2020) and ERT (blue) profiles in Golyam Kazan area. Error in horizontal coordinates of the profiles is $1-2\ m$. Bold red lines show the position of frozen subsurface areas, and bold blue lines show place of melt water (subsurface drainage system).

of distance makes it possible to increase the depth of the subsurface study. In our study, a maximum depth of $9-10\ m$ is reached, and for most of the profiles the expected depth at this length of the measuring line with a multi-electrode system with 24 electrodes using the fore-electrode symmetric Schlumberger array, was $6-7\ m$. The selected length of the profiles and the type of measuring scheme were in accordance with the conditions on the field, and the impossibility of applying a three-electrode (pole-dipole array) or dipole-dipole array measuring scheme. The lengths of the profiles were chosen to have

https://doi.org/10.5194/tc-2021-337
Preprint. Discussion started: 20 December 2021

the maximum length (through the whole microglacier bed) and depth of study, while not having to cross over moraine ridge of the glacier (which was unstable and dangerous for climbing). Profiles are around $30-40\ m$ long with north-south direction and electrode spacing of $1.5\ m$.

ERT measurements near Snezhnika were conducted in 2018, 2019 and in 2020 along one, two and three profiles respectively. They were situated in the lower part of the microglacier bed on the free from ice and snow area (depending on the size of microglacier in the respective year Fig. 2). Thus the first profile was measured all three years, the second twice and the third only in 2020 (Fig. 3). The last profile crosses small part of the microglacier. A pseudo-section of the apparent resistivity for each profile was obtained, consisting of the measured values at certain points along horizontal lines at a certain depth. To transform it into a real geoelectrical section, we used the algorithm for two-dimensional inversion by the method of least squares, proposed by Loke et al. (1996), implemented by quasi-Newtonian optimization.

3 Results and discussion

3.1 Geophysical investigations of Snezhnika microglacier

The thickness and internal structure of Snezhnika microglacier were investigated using GPR. The obtained GPR data were used to acquire nine radargrams, which were analyzed and interpreted and are presented on Fig. 4, Fig. 5, Fig. 6. Across seven radagrams the discontinuity between the microglacier's ice and bed is well visible. The other two profiles were made in the lowest part of microglacier's bed in a free from ice area and respectively the discontinuity is not presented.

On the Fig. 4 are presented radargrams from 2018, which are horizontal relative to the slope. The snowfield is situated in a very steep area and this made measurements in its upper part very difficult. The uppermost layer represents the microglacier. Its depth varies between $1-2\ m$ in the lowest part (Fig. 4a) and $5-6\ m$ on the last profile (Fig. 4e). Within the ice, there are some less differentiated discontinuities, probably related to the structural features of the ice body. For this layer an average ice velocity of $V_{ice} = 0.15\ m/ns$ was used (Baker et al., 2007). The place of profiles GPR(2018)-1, GPR(2018)-2 and partially GPR(2018)-3 (Fig. 4a,b and c) was not covered by snow in previous year (Fig. 2a) so the first layer of these three profiles, respectively, is actually the "new" snow left over from the last winter.

The second layer lies under the ice, representing the glacial bed of rock blocks of different sizes, the voids between which are filled with ice and water. We presume that this layer is draining the melted glacial water. The thickness of this layer varies from 1 to $4\ m$ along the particular lines and its depth is between $3.5-6\ m$ on the first profile (Fig. 4a) and $5-8\ m$ on the last one (Fig. 4e). An average layer velocity of $V_{gravel} = 0.13\ m/ns$ is used.

The third layer has a complex topography in the lower elevation survey lines, while in the higher elevation lines (GPR(2018)-03, GPR(2018)-04 and GPR(2018)-05, Fig. 4 c,d and e) it becomes almost parallel to the one above with a thickness of $4-6\ m$. In the first and second survey line (GPR(2018)-01 and GPR(2018)-02), the layer is relatively thin in its central part (about $1\ m$), while two pocket-like recesses with thickness of up to about $6-7\ m$ (and depth $10-12\ m$ from the ground level) are formed along the left and the right part. The presence of ice causes some distortion of the signal due to large differences in the velocity

https://doi.org/10.5194/tc-2021-337
Preprint. Discussion started: 20 December 2021

of electromagnetic waves in dry and icy areas. Based on this we assume that the pocket-like structures are ice lenses. The intermediate layer velocity used in the interpretation is $V_{limestone} = 0.12\ m/ns$.

Pale rectangular areas are visible on the radargrams. Most visible they are on the higher elevation profile (GPR(2018)-05, Fig. 4e). They have no scientific meaning and exist due to technical reasons. Due to the steep slope in the upper part of the microglacier the measurements were stopped and started several times and this caused gain level changes in some places.

On Fig. 5 profiles GPR(2020)-1 and GPR(2020)-2 along the slope of Snezhnika are presented (Fig. 3). Both profiles are plotted horizontally in order to present better the discontinuities, although there is a change in elevation of 24 m between start and end point of each profile. In the both radargrams only the ice layer can be seen.

The first profile (GPR(2020)-1, Fig. 5a) clearly outlines the lower surface of the snowfield with a depth of between 4 and $7\ m$. At the beginning of the profile (left part of radargram), fading of the phases is observed at a greater depth ($> 7\ m$), which may be due to a frozen zone beneath the upper part of the microglacier. In the first half of the radargram a hill-like structure is visible, which can be interpreted as plucking zone of the microglacier. On the right part of the profile the discontinuity between the microglacier's ice and the bed has the greatest depth of $7\ m$, which becomes shallower at the end of the profile, in the last $4-5\ m$ of it. Beneath lowest part of the microglacier another hill-like structure is visible. It can be interpreted as the new head moraine.

In the second profile (GPR(2020)-2, Fig. 5b), the relief of the lower surface is clearly traced at a depth of about $8\ m$. Here a layer with a depth of 4 to $8\ m$ is distinguished, which is composed of either frozen and well-joined rock blocks or older ice. At the lower end of the profile (right part of the radargram), single reflections can be seen in this layer, which are probably due to larger pieces of rock covered by ice.

The obtained depths of the Snezhnika in 2020 correlate very well with the results obtained in 2018. At that time, the depth in the uppermost profile is about $6-7\ m$ (Fig. 4e). Profile GPR(2020)-1 intersects profiles GPR(2018)-4 and GPR(2018)-5 and as can be seen from Fig. 3 and Fig. 5a the place of intersection is also the place of the greatest thickness, with a depth of $7\ m$. The deepest part of microglacier is detected on GPR(2020)-2, where the thickness of the ice is $8\ m$. This profile is located in the southern part of microglacier, which is most shaded by Vihren wall and Dzhamdzhiev ridge (Fig. 2e). The obtained maximal thickness of microglacier shows agreement with results from early borehole measurements conducted by Popov (1962). The depth of 11 m (Gruenewald et al., 2008) is not detected even with wider aerial information obtained from geophysical measurements. We have to notice that borehole measurements of depth give only point information, compared to the profile measurements, and not the whole area of microglacier was covered by GPR profiles in years 2018 and 2020.

The main layers outlined in the study area are also presented in Table 2.

3.2 Subsurface structure of microglacier bed

Subsurface structure of microglacier bed was investigated using ERT and GPR measurements. On Fig. 6 are presented two GPR profiles from 2020, located in the lowest part of the area (Fig. 3). A change in elevation between these horizontal relative to the slope profiles can be observed, which is due to the topographic correction during the GPR data processing. The elevations are taken mainly from topographical maps in scale 1:5000, from DEM based on aerial photography and GPS data. In the presence

https://doi.org/10.5194/tc-2021-337
Preprint. Discussion started: 20 December 2021


The Cryosphere Discussions

Table 2. Description of the stratigraphy of the study area.

Layer	Depth	Thickness	Description
1. Microglacier	From $1-2\ m$ in the lowest part and up to $7-8\ m$ in the higher part	2 to 8 m	The top layer combines the inner sublayers and discontinuities of the microglacier
2. Glacial bed	Between $3.5-6\ m$ in the lowest part and $5-8\ m$ in the upper parts of the slope	1 to 4 m	Rock blocks of different size with voids and channels between them filled with ice and water
3. Permafrost	7 to 9 m in the lower parts of the relief with two pocket-like recesses up to $7-9\ m$ and between $11-13\ m$ in the higher parts	1 to 8 m	Permafrost zone with two ice lenses along the left and the right side under the glacial bed of the microglacier
4. Bedrock	$>$ 14 m	$>$ 10 m	Fractured marble rocks massif

of relatively uniform inclination of the profile line relief is introduced as a linear function of the start and end points of the profiles.

The two GPR profiles situated in the glacial bed were also covered by ERT measurements. Fig. 7 shows pseudo-section of the apparent resistivity for profile ERT-PR1, measured in 2018, 2019 and 2020. On the resulting plot, three zones can clearly be distinguished. Zone-1 is situated near the surface and represents gravel with different size of rocks (between 1 mm and $15-20\ cm$) It characterized by a relatively high electrical resistivity of 8000 to 40000 Ωm which is typical for broken marble rocks (Dortman, 1984). In 2018 (Fig. 7c) the thickness of this zone is $1.5-2\ m$, and in the next two years it reaches up to 4 m (Fig. 7a and b). Below the first zone, at a depth of 1 to 5 m, the second zone is located (Zone-2). It is characterized by relatively low values of the specific electrical resistivity within the range of 1000 to 8000 Ωm. This zone represents a highly watered zone, draining the melting microglacier water. Its size is smaller in 2018 and is located mainly in the edges of glacial bed on a depth of 3 m. In the next two years its size increases and its thickness decreases to 2 m. The deepest zone (Zone-3) is of the greatest interest and is characterized by resistivity over 60000 Ωm. High resistivities (Kneisel et al., 2008; Hauck et al., 2001) are typical for ice and frozen subsurface. Based on this we assume that the zone represents a frozen area.

In the second electrical profile (ERT-PR2), presented on Fig. 8, we distinguish two zones. Zone-2 is located in nearsurface area of the profile, with a thickness up to 2 m. This area represents the accommodating medium composed of crushed marble pieces of different sizes, having a resistivity between 10000 and 40000 Ωm. The zone is highly watered and is a result from melting of the microglacier. In the southern part of the profile at a depth beyond the third meter in the section Zone-3 is located. This zone appears with values of electrical resistivity over 60000 Ωm and represents a frozen area in the base of microglacier. In 2020 (Fig. 8 down) the frozen area is located about 1 m deeper than in 2019 (Fig. 8 up).

https://doi.org/10.5194/tc-2021-337
Preprint. Discussion started: 20 December 2021

Fig. 9 shows the third ERT profile (ERT-PR3), located just below the glacier. This profile was measured only in 2020 when the size of Snezhnika was the smallest. The measuring line passed through a small piece of the snowfield, which is well seen on the Figure. Zone-3, representing again the ice area in the base of the microglacier, occupies a large part of the section. It is located at a depth of $4\ m$ in the southern part of the profile and in the northern it reaches the surface. Namely the northern part of the profile crosses part of the glacier (Fig. 3). Zone-2 on ERT-PR3 is distinguished only in the very shallow parts of the profile.

The frozen subsurface area and zone of draining water are better seen when we compare radargrams and ERT plots. Comparison is presented on Fig. 11 and Fig. 10.

On the resulting plot for ERT-PR1 and GPR(2020)-3, frozen and watered zones can clearly be distinguished (Fig. 10). Position of these zone on radargram is shown by arrows. The watered zones have low values of resistivities and more reflections on GPR profile. They represents areas formed by the melting of the glacier, mixed with crushed rock material. Between them is situated a zone characterized by high resistivities of more than $60000\ \Omega m$ on ERT plot and a phase fading on GPR plot, representing the frozen area at the base of the microglacier.

Figure 11 shows ERT-PR2 profile measured in 2019 (up, left) and in 2020 (down, left) and GPR(2018)-1 and GPR(2018)-2 profiles. Snow layer from 2018 is well visible on the radargrams (right on the figure) and the surface beneath the snow has the same shape on the ERT profiles without snow. ERT data cover smaller area in depth than GPR although the high resistivity zone fits well with the area of frozen zone interpreted on GPR profiles.

The frozen zone is situated mainly in the southern part of the microglacier's bed (Fig. 3). Also, the southern part of the microglacier is at least 1 m thicker than the northern one (Fig. 5). The reason is that this part is closer to Dzhamdzhiev ridge and the wall of the Vihren peak - both with very steep slopes and rising 300 - 400 m above the surface. They shade the Snezhnika for most of the day even in the sunniest days of summer, as seen from Fig 2e. The picture is taken namely from Dhamdzhiev ridge on 1. July in the middle of the day and the shadow over the southern part of the microglacier can already be observed. The shading effect causes the northern part of the area to be exposed to the sun longer than the southern part. During the summer this protects the microglacier and the frozen area from high temperatures. Proof of this assumption is the presence of snow patches, located at the bottom of the Dzhamdzhiev ridge, close to the Snezhnika. Snow patches were no observed in the northern part of the cirque. From the other side, no frozen zone was obtained near the perennial snow patch located in the middle of the Banski Suhodol valley, Pirin Mountain (unpublished research of the authors). The valley is situated northern from Golyam Kazan cirque and is more wider than it, thus the shading from the surrounding mountain ridges is less.

The frozen zone in Golyamm Kazan cirque was obtained in 2018 on the ERT profile and in GPR profiles PR(2018)-1 and GPR(2018)-2. The results from 2020 are showing again indications of a frozen area below the surface, although its lower part is not discovered at the same depth as in 2018. The reason for this is the smaller size of Snezhnika in 2020 compared to 2018. The perennial snow patch preserves the frozen subsurface area in summer. Even when the size of the microglacier is smaller, a frozen zone exists but is observed more deeply. The shading of surrounding mountain ridges is less effective than protection of snowpatch, but it is very important.

https://doi.org/10.5194/tc-2021-337
Preprint. Discussion started: 20 December 2021

The study presented includes measurements made over three consecutive years and a frozen zone is observed every year. According to the definition of permafrost (Harris et al., 1988) this can be treated as evidence of permafrost existence in high mountains (particularly Pirin Mountain) of Bulgaria.

4 Conclusions

Detailed geophysical measurements of Snezhnika microglacier in Golyam Kazan, Pirin were conducted in 2018, 2019 and 2020 in order to estimate the thickness and internal structure of the snow body and subsurface structure beneath and near it. The mean thickness is estimated from radargrams as about $4-6\ m$. In some places in the southern part of the ice body it reaches $8\ m$. The estimated thickness shows partly agreement with the results from early borehole measurements and results obtained by Popov (1962) but the depth of 11 m (Gruenewald et al., 2008) is not detected. Our GPR measurements cover large but not the whole area of the microglacier and borehole measurement of the depth give information only in one point from the area. We assume that this is the reason of disagreement with the estimated from (Gruenewald et al., 2008) thickness. It is still not possible to estimate the changes in thickness of the microglacier through the years starting from 1962 due to insufficient data. However the obtained results for the thickness are good base for future monitoring of microglacier not only by size.

The underlying layer is the glacial bed and consists of rock blocks of different sizes between which are filled with ice and water and voids. This layer is likely draining the melted glacial water, which is important for preservation of the snow patch. Microglacier drainage systems is fully situated beneath the surface as no or rare observed is surface water in Golyam Kazan cirque. The thickness of this layer varies from 1 to $4\ m$ along the particular lines.

GPR and ERT measurements were made also near Snezhnika microglacier. On the lowest situated GPR profiles from 2018 a zone with complex relief is distinguished. The zone is located in the southern part of the microglacier and reaches the head moraine. ERT profiles show an anomaly at the same place with very high resistivity, $\geqslant 60000\ \Omega m$. Such values are typical for ice. The high vales of resistivity and the lack of reflections on the GPR profiles give us a reason to conclude that the zone represents a frozen area. ERT measurements were repeated in the next two years and the anomaly is observed all consecutive years. Based on this we can also assume that we have evidences of permafrost in Pirin mountain.

The frozen zone is situated in the southern part of the microglacier and exists beneath the ice and without ice cover as in late autumn of 2020, when the microglacier's size was smallest and no shading of the ice layer was possible. The area is closer to the Dzhamdzhiev ridge and is shaded from it for the most of the day in the summer. This result suggest the importance of mountain ridge shading for the preservation of frozen subsurface areas in the Golyam Kazan cirque, Pirin Mountain. The assumption is also supported by the fact that no frozen zone was obtained near the perennial snow patch in Banski Suhodol valley, where the snow field is in the middle of the valley and far less protected by shading from the surrounding mountain ridges.

https://doi.org/10.5194/tc-2021-337
Preprint. Discussion started: 20 December 2021

Data availability. Authors are happy to share data requested by email. Available data is: GPR data from Golyam Kazan (2018 and 2020); ERT measurements in Golyam Kazan (2018, 2019 and 2020); GPS tracks of snowfields and photos.

Author contributions. AK led ERT measurements and processed the data. CT led the GPR measurements and processed the data. GG led the projects and organized the field work. GG prepared the manuscript with contribution of all co-authors.

Competing interests. The authors declare that they have no conflict of interest.

https://doi.org/10.5194/tc-2021-337
Preprint. Discussion started: 20 December 2021

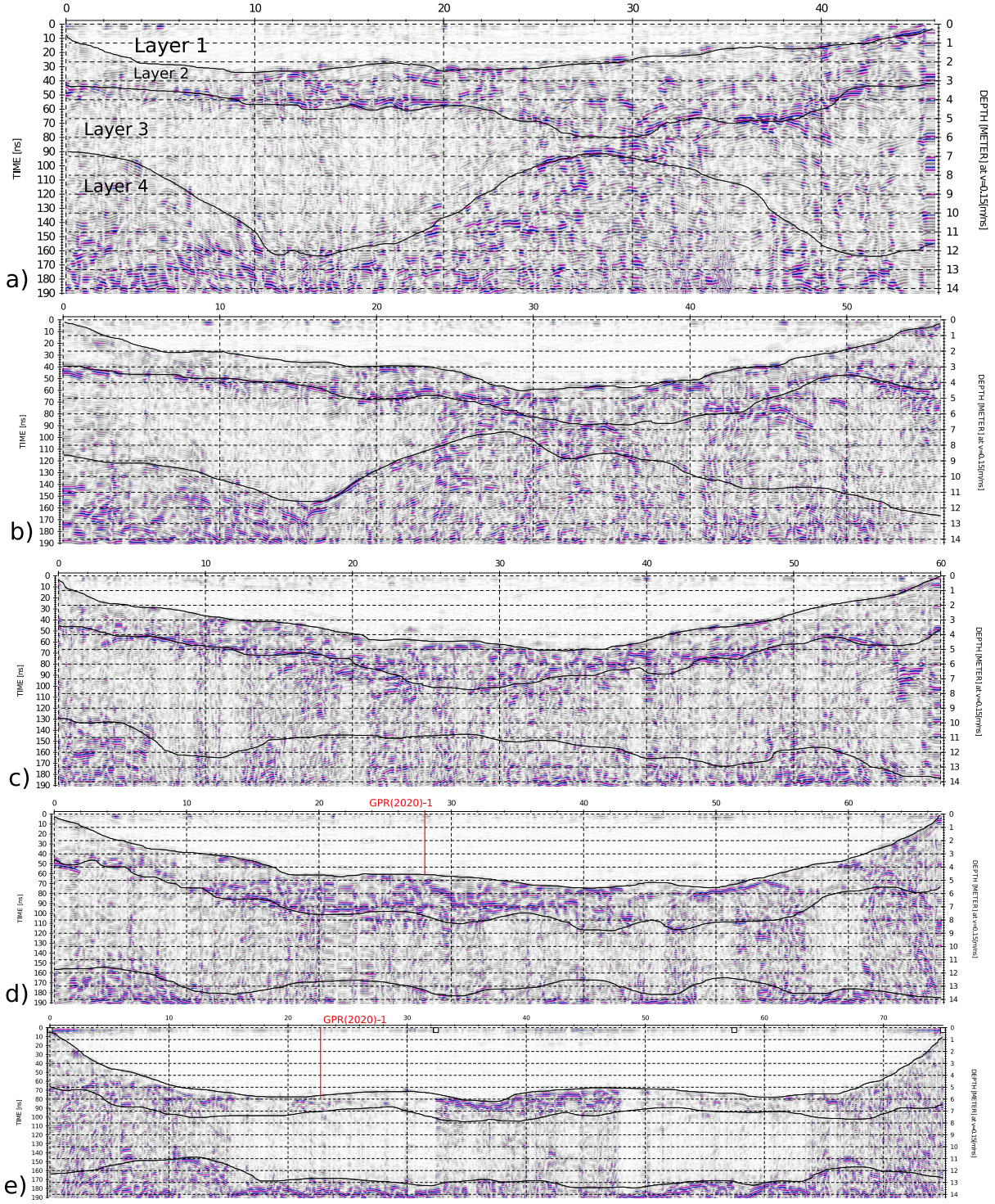

Figure 4. GPR profiles from 2018: a) GPR(2018)-1 situated at lowest altitude; b) GPR(2018)-2; c) GPR(2018)-3; d) GPR(2018)-4; e) GPR(2018)-5 situated at highest altitude. All profiles are with horizontal elevation. Red lines indicate the coss point with GPR(2020)-1.

https://doi.org/10.5194/tc-2021-337
Preprint. Discussion started: 20 December 2021

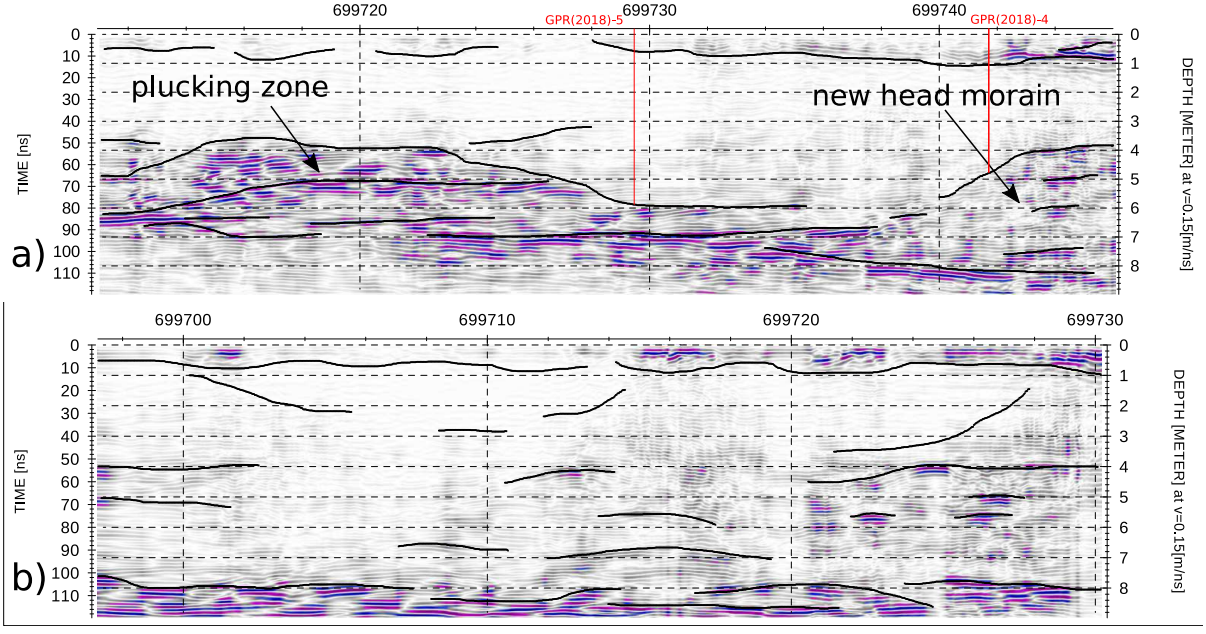

Figure 5. GPR profiles from 2020 along the slope of Snezhnika: a) GPR(2020)-1 north; b) GPR(2020)-2 south. Radargrams are plotted horizontally, but a change in elevation of 24 m between start (left) and end (right) point of each profile exists. Red lines indicate the cross point of GPR(2020)-1 with GPR(2018)-4 and GPR(2018)-5.

https://doi.org/10.5194/tc-2021-337
Preprint. Discussion started: 20 December 2021

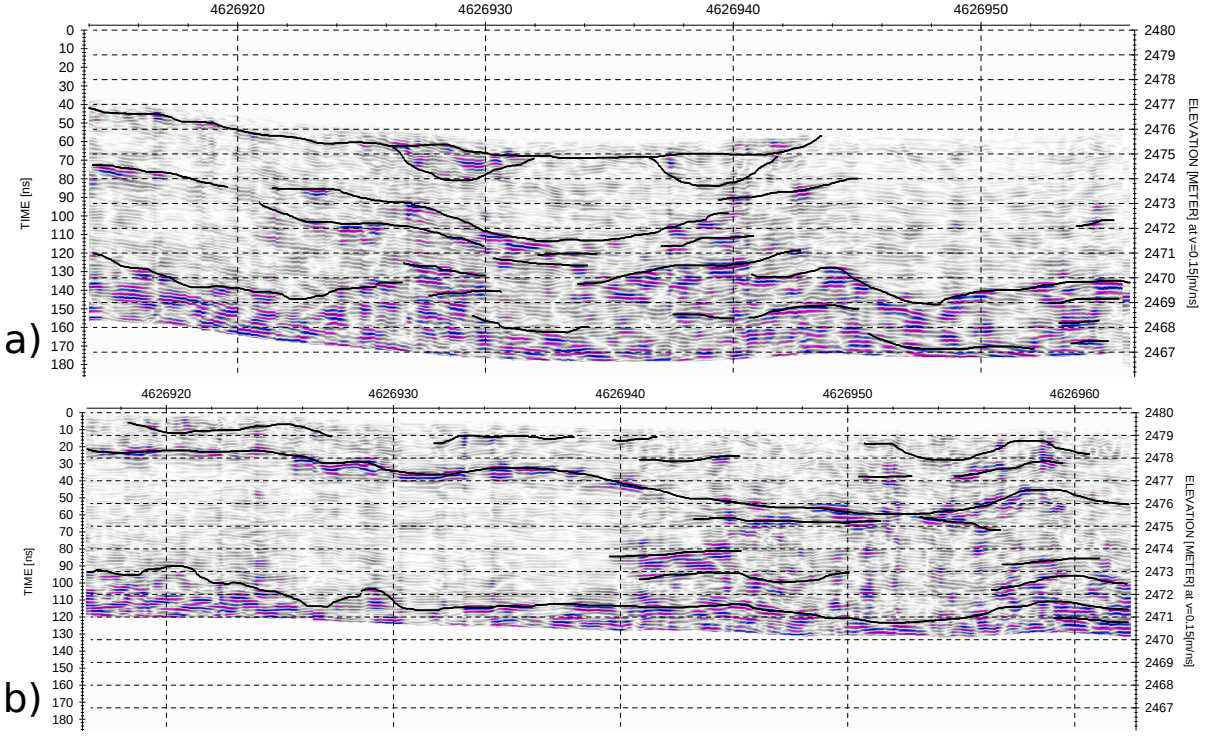

Figure 6. GPR profiles from 2020 situated in glacial bed near the head moraine: a) GPR(2020)-3; b) GPR(2020)-4.

https://doi.org/10.5194/tc-2021-337
Preprint. Discussion started: 20 December 2021

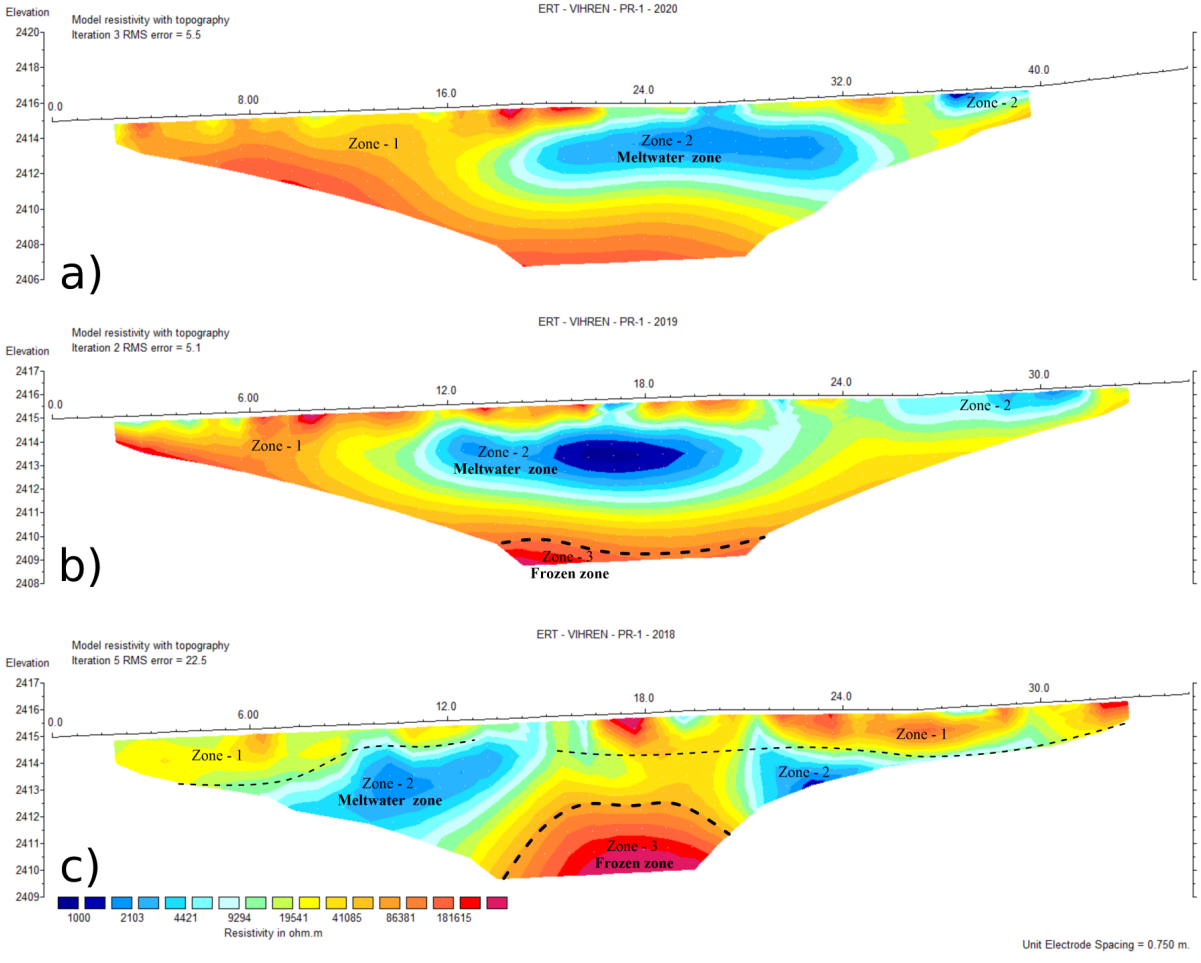

Figure 7. Electrical resistivity sections along ERT-PR1 obtained near Snezhnika microglacier in 2020 (a), 2019 (b) and 2018 (c). Blue color represents low resistivities and red color indicates areas with very high resistivities.

https://doi.org/10.5194/tc-2021-337
Preprint. Discussion started: 20 December 2021

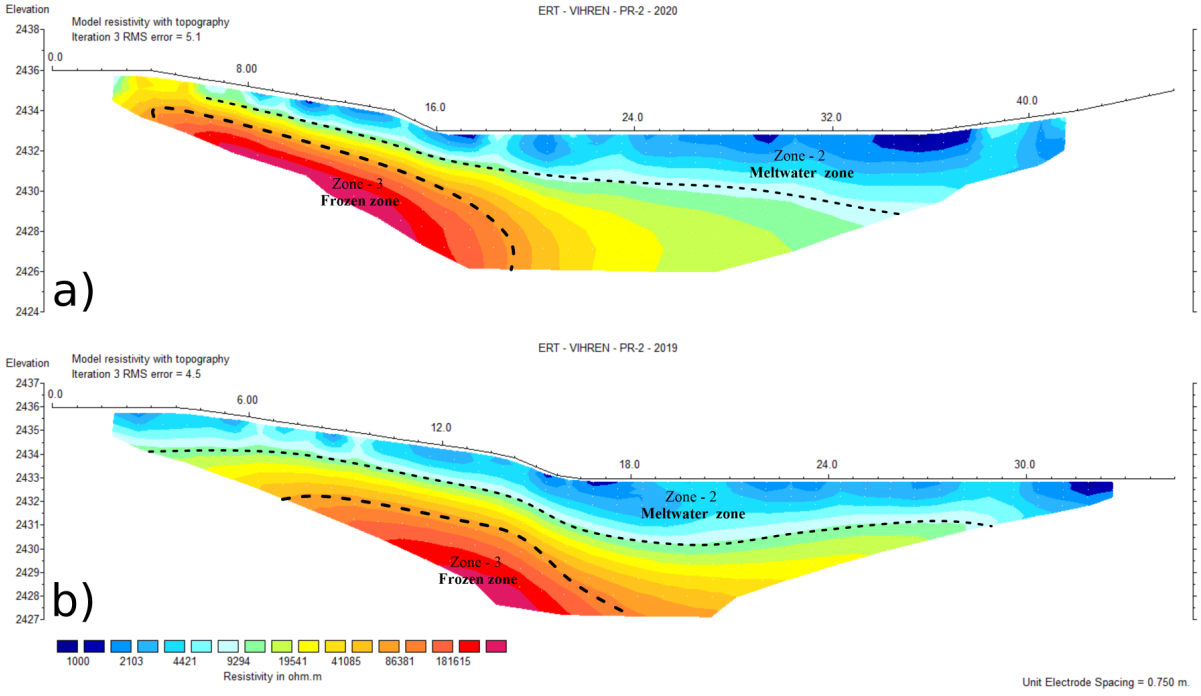

Figure 8. Electrical resistivity sections along ERT-PR2 obtained in Golyam Kazan area in 2020 (a) and 2019 (b).

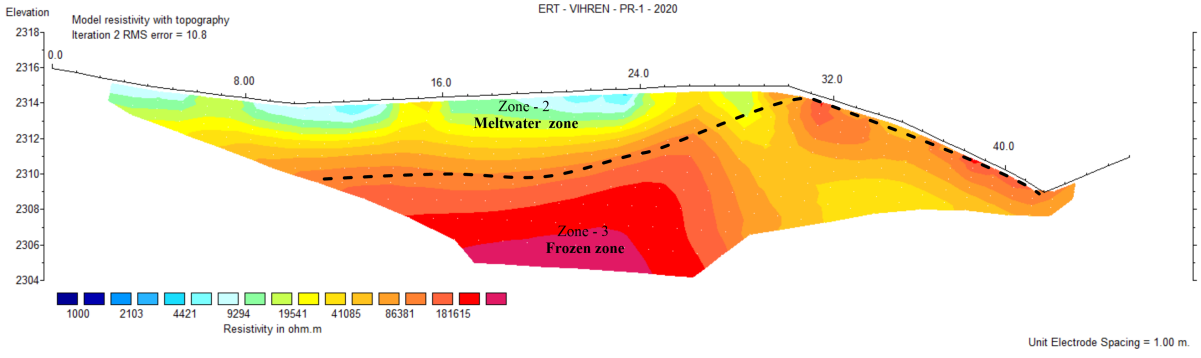

Figure 9. Electrical resistivity sections along ERT-PR3 obtained in Golyam Kazan area in 2020.

https://doi.org/10.5194/tc-2021-337
Preprint. Discussion started: 20 December 2021

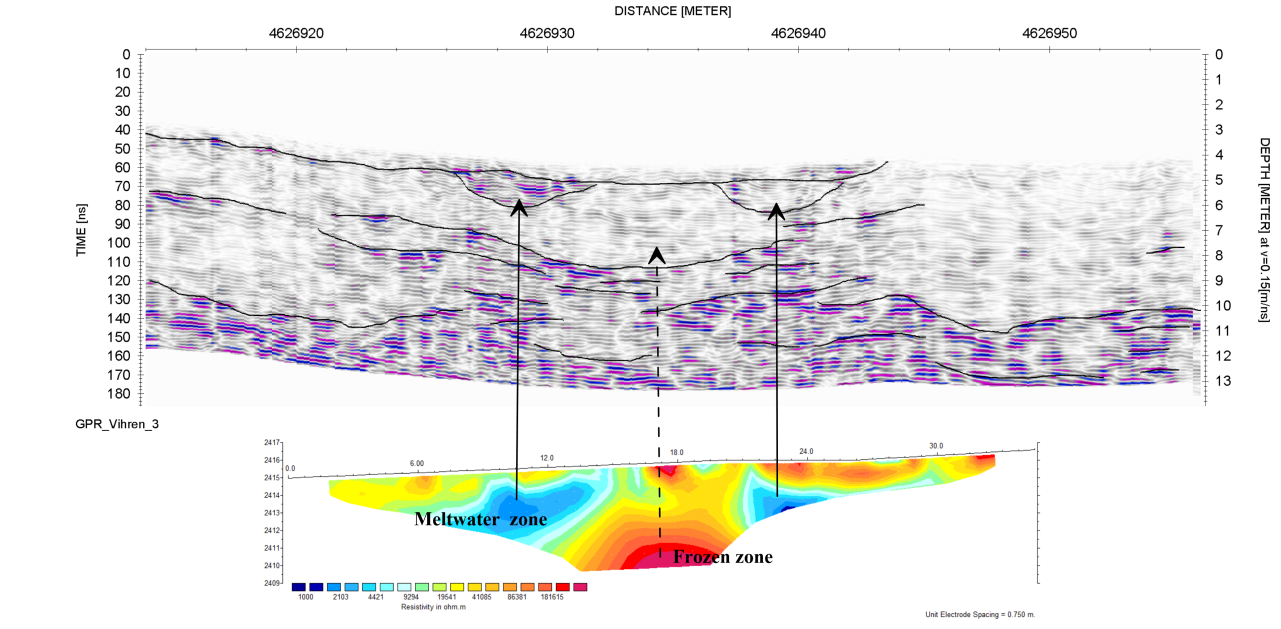

Figure 10. ERT-PR1 and GPR(2020)-3 profiles. Black arrows show water channel. Dashed arrow shows frozen area.

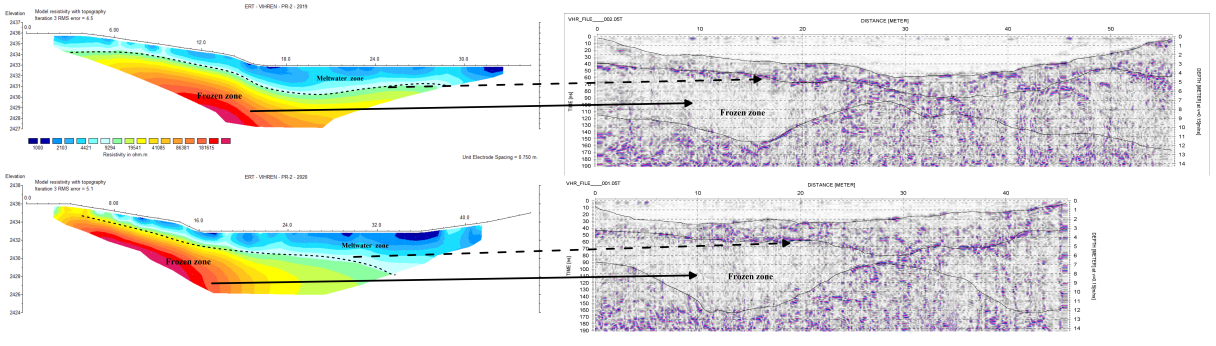

Figure 11. ERT-PR2 and ERT-PR2 profiles and GPR(2018)-1 and GPR(2018)-2 profiles from 2018. Black arrows show the frozen zone.

https://doi.org/10.5194/tc-2021-337
Preprint. Discussion started: 20 December 2021

Acknowledgements. The work was supported by the Science Fund of Sofia University within the projects 80-10-126/21.04.2017, 80-10-217/26.04.2018 and 80-10-24/18.03.2020 and Science Fund of University of Mining and Geology within the project GPF-222/11.03.2019. All measurements were carried out with the participation of students from both universities. The authors thank the following students: Boriyana Chtirkova, Bojourka Georgieva, Daniel Ishlyamski, Dragomir Dragomirov, Yanko Ivanov, Spas Nikolov, Valentin Buchakchiev, Kalina Stoimenova and Angel Dimitrov. We thank also Vassil Gourev for sharing idea and knowledge of studying perennial snow patches in Bulgarian mountains. Measurements were performed with the permission of Pirin National Park administration.

https://doi.org/10.5194/tc-2021-337
Preprint. Discussion started: 20 December 2021

References

Annan, P., J. Davis. Impulse radar sounding in permafrost. Radio Science, 11 (4), pp. 383-394, 1976

Arcone, S.A. High Resolution of Glacial Ice Stratigraphy: A Ground-penetrating Radar Study of Pegasus Runway, McMurdo Station, Antarctica. Geophysics, 61, 1653–1663, 1996

Arcone, S.A., Lawson, D.E., and Delaney, A.J., Short-pulse radar wavelet recovery and resolution of dielectric contrasts within englacial and basal ice of Matanuska Glacier, Alaska. Journal of Glaciology, Vol. 41, pp. 68–86, 1995

Baker, G. S., T. E. Jordan, J. Pardy, An introduction to ground penetrating radar (GPR), Stratigraphic Analyses Using GPR, Geological Society of America DOI = 10.1130/SPE432, ISBN print: 9780813724324

Barry, R. & Gan, T.Y. The global cryosphere: past, present and future. Cambridge University Press, Cambridge, 2011

Berthling, I., Etzelmuller, B., Isaksen, K. and Sollid, J.L., Rock glaciers on Prins Karls Forland. II: GPR soundings and the development of internal structures. Permafrost and Periglacial Processes, 11 (4), 357-369, 2000

Blindow, N., The central part of the Filchner-Ronne Ice Shelf, Antarctica: Internal structures revealed by 40 MHz monopulse RES. Annals of Glaciology, Vol. 20, pp. 365–371, 1994

Boyadjiev, S. On the geology of Pirin Mountain. Annuaire de la Direction des Recherches Geologiques et Minieres 8, 89–125, 1959 (in Bulgarian)

Damm, B., & Langer, M. Kartierung und Regionalisierung von Permafrostindikatoren im Rieserfernergebiet (Südtirol/Osttirol). Mitteilungen der Österreichischen Geographischen Gesellschaft, 148, 295-314, 2006

Dimovski, S., Stoyanov, N., Gyurov, C., Efficiency of electromotography for detailed geoelectrical mapping of nearsurface geological section, Bulaqua, 4, pp. 47-55, 2007

Dimovski, S., Stoyanov, N., Localization of suitable sites for the construction of monitoring wells in a small-scale rock complex, Annual of University of Mining and Geology ”St. Ivan Rilski”, 58(1), 140–145, 2015

Dobinski, W., Permafrost of the Carpathian and Balkan Mountains, eastern and southeastern Europe. Permafrost Periglac. Process., 16: 395-398, 2005. DOI = 10.1002/ppp.524

Dortman, N. B. Physical Properties of the Rocks and Mineral Resources. Handbook of the Geophysicist. Nedra, Moscow, 1984. (in Russian)

Emmert, A., Ch. Kneisel (2017) Internal structure of two alpine rock glaciers investigated by quasi-3-D electrical resistivity imaging. The Cryosphere, 11, 841–855, 2017

Evans, S. Dielectric properties of ice and snow - a review. Journal of Glaciology, Vol. 5, No. 42, p. 773-92, 1965

Fitzgerald, W.J., and Paren, J.G. The dielectric properties of Antarctic ice. Journal of Glaciology, Vol. 15, No. 73, p. 39-48, 1975

Fort M., Impact of climate change on mountain environment dynamics, Journal of Alpine Research, 103-2, DOI = 10.4000/rga.2877, 2015

Gadek, B., Grabiec, M. Glacial ice and permafrost distribution in the Medena Kotlina (Slovak Tatras): mapped with application of GPR and GST measurements. STUDIA GEOMORPHOLOGICA CARPATHO-BALCANICA, VOL. XLII, 5–22, 2008

Gachev, E., Climatic factors for the year-round dynamics of microglacier Snezhnika in Pirin, Scientific conference ”Geographic aspects of planning and the use of the territory in the context of global changes”, Extended Abstracts, 2016 (in Bulgarian)

Gachev, E., Stoyanov, K., Gikov, A. Small glaciers on the Balkan Peninsula: State and changes in the last several years. Quaternary International 415. DOI = 10.1016/j.quaint.2015.10.042, 2016

Gachev, E. The Unknown Southernmost Glaciers of Europe. Glaciers evolution in a changing world. Zagreb. DOI = 10.5772/intechopen.68899, 2017a

https://doi.org/10.5194/tc-2021-337
Preprint. Discussion started: 20 December 2021

Gachev, E. High mountain relief in marble in Pirin mountains, Bulgaria: Structure, specifics and evolution. Rev.Geomorfol., 19, 118-135, 2017b

Gachev, E., Gikov, A., Zlatinova, C., Blagoev, B. Present state of Bulgarian glacierets. Landform Analysis, 11, 16-24, 2009

Gachev, E., Gikov, A. Description and first measurement of the snowfield in the Banski Suhodol circus. Problems of geography, 3-4. 90-98, 2010

Georgieva, G., Kisyov, A., Tzankov, C., Chtirkova, B., Gourev, V., Ivanov, Y., Evaluation of geophysical methods for studying snowfields in Pirin Mountain, Bulgaria Extended abstract from 10th Congress of Balkan Geophysical Society, BGS 2019. DOI = 10.3997/2214-4609.201902662, 2019

Gruber S., Haeberli W. Mountain Permafrost. In: Margesin R. (eds) Permafrost Soils. Soil Biology, vol 16. Springer, Berlin, Heidelberg. DOI = 10.1007/978-3-540-69371-0_3, 2009

Grünewald K., Weber C., Scheithauer J. & Haubold, E., Mikrogletscher als Klimaindikatoren und Umweltarchive in sudosteuropaischen Hochgebirgen? - Untersuchung des Vichrengletschers im Piringebirge (Bulgarien). Zschr. Gletscherkunde und Glazialgeologie, 99–114, 2006

Grunewald, K., Scheithauer, J. Klima- und Landschaftgeschichte Sudosteuropas. Rekonstruktion anhand von Geoarchiven im Piringebirge (Bulgarien). Rhombos Verlag, Berlin,178 pp, 2008

Gruenewald, K., Scheithauer, J., Gikov, A., Microglaciers in the Pirin Mountains, Problems of Geography, 1–2, 1–16, 2008 (in Bulgarian).

Grunewald, K., & Scheithauer, J. Europe's southernmost glaciers: Response and adaptation to climate change. Journal of Glaciology, 56(195), 129-142. DOI = 10.3189/002214310791190947, 2010

Grunewald, K., & Scheithauer, J. Europe's southernmost glaciers: response and adaptation to climate change. Journal of glaciology, 56(195), 129-142, 2010

Guodong, C. and Dramis F., Distribution of mountain permafrost and climate. Permafrost and Periglacial Process., 3, 83-91, 1992

Harris, S. A.; French, H. M.; Heginbottom, J. A.; Johnston, G. H.; Ladanyi, B.; Sego, D. C.; van Everdingen, R. O., Glossary of permafrost and related ground-ice terms, Technical Memorandum (National Research Council of Canada. Associate Committee on Geotechnical Research), no. ACGR-TM-142,159 p. DOI = 10.4224/20386561, 1988

Hughes, P.D. Little Ice Age glaciers in the Mediterranean mountains. Mediterranee, 122, 63-79, 2014

Hughes, P.D.. Little Ice Age glaciers and climate in the Mediterranean mountains: a new analysis., Cuadernos de Investigación Geográfica, 44.1, 15-45, 2018

Hauck, C., Geophysical methods for detecting permafrost in high mountains, Versuchsanstalt fUr Wasserbau Hydrologie und Glaziologie der Eidgenossischen. Technischen Hochschule Zurich, ISSN 0374-0056, 2001

Hauck, C.: New Concepts in Geophysical Surveying and Data Interpretation for Permafrost Terrain, Permafrost Periglac., 24, 131– 137, doi:10.1002/ppp.1774, 2013.

Hausmann, H., Krainer, K., Brück, E., and Ullrich, C.: Internal structure, ice content and dynamics of Ölgrube and Kaiserberg rock glaciers (Ötztal Alps, Austria) determined from geophysical surveys, Austrian Journal of Earth Sciences, 105, 12–31, 2012.

Haeberli, W., Untersuchungen zur Verbreitung von Permafrost zwischen Flüelapass und Piz Grialetsch (Graubünden). Mitteilung der Versuchsanstalt für Wasserbau, Hydrologie und Glaziologie, 1975, 18, 7-128.

Hilbich, C.,Marescot, C. L. Hauck, C., Loke, M. H., Mäusbacher, R., Applicability of Electrical Resistivity Tomography Monitoring to Coarse Blocky and Ice-rich Permafrost Landforms. Permafrost and Periglacial Processes 20(3): 269-284, 2009

https://doi.org/10.5194/tc-2021-337
Preprint. Discussion started: 20 December 2021

Hinkel, K.M., J.A. Doolittle, J.G. Bockheim, F.E. Nelson, R. Paetzold, J.M. Kimble, R. Travis. Detection of subsurface permafrost features with ground-penetrating radar, Barrow Alaska Permafrost and Periglacial Processes, 12, pp. 179-190, 2001

Hoekstra, P. & McNeill, D. Electromagnetic probing of permafrost. In North American Contribution, Second International Conference on Permafrost, Yakutsk, USSR (pp. 517–526). Washington DC: National Academy of Sciences, 1973

Hoekstra, P. & Delaney, A. Dielectric properties of soils at UHF and microwave frequencies. Journal of Geophysical Research Journal of Geophysical Research, 79(11), 1699–1708, 1974

Ikeda, A.: Combination of conventional geophysical methods for sounding the composition of rock glaciers in the Swiss Alps, Permafrost Periglac., 17, 35–48, doi:10.1002/ppp.550, 2006

Ingeman-Nielsen, T., Geophysical techniques applied to permafrost investigations in Greenland. Ph.D. Thesis BYG DTU R-123 Arctic Technology Centre Department of Civil Engineering Technical University of Denmark, ISSN 1602-2917, 2005

Jol, Harry M. (Editor), Ground Penetrating Radar Theory and Applications (1st Edition). Elsevier, p. 544. ISBN 9780444533487 7, 2009

Jørgensen, A. S., F. Andreasen. Mapping of permafrost surface using ground-penetrating radar at Kangerlussuaq Airport, western Greenland. Cold Regions Science and Technology, 48, 1, 64-72, 2007

Kawashima, K., Yamada, T., & Wakahama, G. Investigations of internal structure and transformational processes from firn to ice in a perennial snow patch. Annals of Glaciology, 18, 117-122. DOI = 10.3189/S0260305500011368, 1993

King, M. S. The influence of clay-sized particles on seismic velocity for Canadian Arctic Permafrost. Canadian Journal of Earth Sciences, 21(1), 19–24, 1984

King, M. S., Zimmerman, R. W., & Corwin, R. F. Seismic and electrical properties of unconsolidated permafrost. Geophysical Prospecting, 36(4), 349–364, 1988

Kisyov,A., Tzankov, Ch., Chtirkova, B., Georgieva, G., Ivanov, Y., Georgieva, B., Ishlyamski, D., Gourev, V., Nikolov, S., Study of perennial snow patches in Bulgaria, Proceedings of IX National Geophysical Conference, 2018, Sofia (In Bulgarian)

Kneisel, C. & Kääb, A.: Mountain permafrost dynamics within a recently exposed glacier forefield inferred by a combined geomorphological, geophysical and photogrammetrical approach, Earth Surf. Proc. Land., 32, 1797–1810, doi:10.1002/esp.1488, 2007

Kneisel, C., Hauck, C., Fortier, R., and Moorman, B.: Advances in geophysical methods for permafrost investigations, Permafrost and Periglacial Process, 19, 157–178, DOI = 10.1002/ppp.616, 2008

Lawson, D.E., Strasser, J.C., Evenson, E.B., Alley, R.B., Larson, G.J. and Arcone, S.A., Glaciohydraulic supercooling: A freeze-on mechanism to create stratified, debris-rich basal ice: I. Field evidence. Journal of Glaciology, Vol. 44, pp. 547-562, 1998

Loke, M. and Barker, R., Rapid leastsquares inversion of apparent resistivity pseudosections by a quasi Newton method. Geophysical Prospecting, 44: 131-152. DOI = 10.1111/j.1365-2478.1996.tb00142.x, 1996

Maurer, H. & Hauck, C.: Geophysical imaging of alpine rock glaciers, J. Glaciol., 53, 110–120, DOI = 10.3189/172756507781833893, 2007.

Milner, A.M., Brown, L.E. & Hannah, D.M. Hydroe-cological response of river systems to shrinking glaciers. Hydrological Processes,23,62–77, 2009

Navarro, F.; Eisen, O. Ground-penetrating radar in glaciological applications. Remote Sens. Glaciers, 195–229, 2009

Olhoeft, G.R., Electrical properties of permafrost. 3nl International Confenmce on Pennafmst, Edmonton. Pmceedings, 1, 127- 131, 1978

Onaca, A., A. C. Ardelean, P. Urdea, F. Ardelean, F. Sîrbu. Detection of mountain permafrost by combining conventional geophysical methods and thermal monitoring in the Retezat Mountains, Romania. Cold Regions Science and Technology, 119, 111-123, 2015

Onaca, A., F. Ardelean, A. Ardelean, B. Magori, F. Sirbu, M. Voiculescu, E. Gachev, Assessment of permafrost conditions in the highest mountains of the Balkan Peninsula, CATENA, 185, 104-288, 2020 ISSN 0341-8162, DOI = 10.1016/j.catena.2019.104288

https://doi.org/10.5194/tc-2021-337
Preprint. Discussion started: 20 December 2021

Pipan, M., Baradello L., Forte E., Prizzon A. Finetti I. 2-D and 3-D processing and interpretation of multi-fold ground penetrating radar data: a case history from an archaeological site J. appl. Geophys., 41, 2-3, 271-292, 1999

Pipan, M., Baradello, L., Forte, E., Prizzon, A. , Polarization and kinematic effects in azimuthal investigations of linear structures with Ground Penetrating Radar, Proceedings of the Symposium on the Application of Geophysics to Engineering and Environmental Problems EEGS, 433-442, 2000

Popov, V., Morphology of the Cirque Golemia Kazan – Pirin Mountains, Announcements of the Institute of Geography, vol. 6, pp. 86-99, 1962 (in Bulgarian)

Popov, V., Observations on the Glacieret in the Cirque Golemia Kazan, the Pirin Mountains, Announcements of the Institute of Geography, Bulgarian Academy of Sciences, vol. 7, pp. 198-207, 1964 (in Bulgarian)

Rolshoven, M., Alpines Permafrostmilieu in der Lasörlinggruppe/ Nördliche Deferegger Alpen (Osttirol)). Polarforschung,1982, 52, 55-64, DOI = 10013/epic.29521

Scott W, Sellmann P, Hunter J. Geophysics in the study of permafrost. In Geotechnical and Environmental Geophysics, Ward S (ed). Society of Exploration Geophysics: Tulsa; 355–384, 1990

Supper, R., D. Ottowitz, B. Jochum, A. Romer1, S. Pfeiler, S. Kauer, M. Keuschnig, A. Ita. Geoelectrical monitoring of frozen ground and permafrost in alpine areas: field studies and considerations towards an improved measuring technology. Near Surface Geophysics, 12, 93-115, 2014

Telford, W.M., Geldart, L.P. and Sheriff, R.E., Applied geophysics. 2nd edition, Cambridge University Press, 1990

van der Kruk, J., Wapenaar, C.P.A., Fokkema, J.T., Van den Berg, P.M. Three-dimensional imaging of multicomponent ground-penetrating radar data Geophysics, 68, 4, 1241-1254, DOI = 10.1190/1.1598116, 2003

Watanabe T. Studies of snow accumulation and ablation on perennial snow patches in the mountains of Japan. Progress in Physical Geography: Earth and Environment. 12(4):560-581. DOI = 10.1177/030913338801200404, 1988

Washburn, A. L. Geocryology - A survey of periglacial processes and environments. University of Washington, 1979

Zemp, M., Glaciers and Climate Change - Spatio-temporal Analysis of Glacier Fluctuations in the European Alps after 1850, Dissertation, Zürich, 2006

Zhao, W., Tian, G., Forte, E., Pipan, M., Wang, Y., Li, X., Shi, Z., Liu, H. Advances in GPR data acquisition and analysis for archaeology Geophys. J. Int., 202, 1, 62-71, 2015

Zhao, W., Forte, E. Colucci, R.R, Pipan, M., High-resolution glacier imaging and characterization by means of GPR attribute analysis, Geophysical Journal International, 206, 2, 1366–1374, DOI = 10.1093/gji/ggw208, 2016